HIGH TEMPERATURE ABSORPTION COEFFICIENTS OF O_2, NH_3, AND H_2O FOR BROADBAND ArF EXCIMER LASER RADIATION

D. F. Davidson, A. Y. Chang, K. Kohse-Höinghaus†, and R. K. Hanson

High Temperature Gasdynamics Laboratory, Department of Mechanical Engineering,
Stanford University, Stanford, CA 94305, U S.A

Abstract—Experimentally-determined absorption coefficients for broadband ArF excimer radiation at 193 mm are presented at temperatures up to 3500 K for O_2, NH_3, and H_2O. These values were determined in a high-purity shock tube, either by measuring excimer pulse fractional absorptions or by measuring photolysis-product yields. Correlations between absorption coefficients and vibrational populations of the absorbing species are discussed. Using these absorption coefficients, a prediction can be made of the amount of O, NH_2, OH, and H produced in shock-tube excimer-photolysis experiments This direct production of radicals is attractive for reaction-kinetics studies in high-temperature gases.

INTRODUCTION

Several questions are raised when excimer lasers are considered as photolysis light sources in high-temperature gas-kinetic studies. Included among these questions are: what are the high-temperature absorption coefficients and the photolysis-product species at excimer wavelengths, and how are the photolysis products distributed over the electronic, vibrational and rotational quantum states and velocity space? Equally important are the questions: how long do these possibly highly non-equilibrium distributions require to relax fully, and what are the effective rate constants for reactions of these non-equilibrium distributions? A complete analysis of photolysis phenomena in high-temperature gas kinetic studies must address these concerns. For rate constants determined using photolysis schemes, knowledge of the distribution of states of the reactant species is essential and this knowledge is in part based on an understanding of the absorption coefficients at elevated temperatures.

Accurate values of absorption coefficients and dissociation quantum yields would be useful in the quantitative production of radicals for chemical kinetic studies. Photolysis work in shock tubes using flashlamps (FPST) and employing only a qualitative understanding of the photolysis products has been described previously.[1,2] These investigations were primarily rate-coefficient determinations performed at long (150–1000 μsec) reaction times. FPST has been used to determine not only the kinetic constants but also the heats of formation of transient species.[3] The first implementation of excimer-laser photolysis in shock-tube experiments was the measurement of the rate of $H + H_2O \rightarrow OH + H_2$ following partial photolysis of H_2O.[4] The use of excimer lasers for photolysis in shock tubes offers prospects for dramatic improvements over previous radical production methods.

Knowledge of excimer wavelength absorption coefficients can also be used in calibrating various diagnostics used in gas phase chemistry. For example, in the case of atomic resonance absorption spectroscopy (ARAS) of species such as H, O, N, and C atoms, accurate calculations for the relevant absorption coefficients of the discharge lamp radiation are presently impossible except in a few cases,[5] and most existing ARAS calibration methods are kinetically or thermodynamically based.[6] Knowledge of the product yields using excimer photolysis provides a known concentration of radicals and hence a reasonably direct method of calibration. In another case, known yields from photolysis of NH_3, using the data presented here, have been used in the calibration of a

†On leave from DFVLR, Institut für Physikalische Chemie der Verbrennung, D-7000 Stuttgart, F.R.G

$NH_2 {}^PQ_{1\ N}(7)$ narrow-linewidth absorption diagnostic in the temperature range of 1500–2200 K, where pyrolysis production of NH_2 from NH_3 was not sufficient to allow a kinetic calibration.[7]

Currently, high-temperature absorption coefficient data at excimer wavelengths are scarce. In one study, the absorption coefficient calculations for ArF excitation of O_2 at moderately high temperatures was verified by measurements done in a heated air torch.[8] In another example, the NH_3 absorption coefficient as a function of temperature from 500 to 2600 K in shock tubes at several u.v. wavelengths was determined.[9] The primary limitation to performing accurate high-temperature absorption coefficient measurements has been the inability to produce a gas mixture hot enough, uniform enough, and without interference absorption to unequivocally determine the absorption coefficients. The shock tube allows for measurements at temperatures in excess of 3500 K and provides a uniform reactant distribution with only one absorber or at least a predictable species concentration uniformity superior to any that is possible with flame absorbers.

Studies of certain simple direct photolysis phenomena have matured to the point that theoretical predictions about product yield and state distribution are possible.[10] Measurements of the high-temperature absorption coefficient for known photolysis wavelength sources enables one to verify these theoretical predictions for certain prepared absorber state distributions, i.e., the Boltzmann distribution in vibrational and rotational energy at various high temperatures. This is, in general, a simpler, though less specific experiment than selectively preparing an individual absorbing state and determining the absorption coefficient and product yields[11]

In this study we describe the determination of absorption coefficients at ArF excimer wavelengths (193 nm) by transmission measurement and by product concentration measurements. A full description of the shock tube photolysis apparatus is presented as well.

EXPERIMENTAL TECHNIQUE

The experimental technique section is divided into four parts: description of the shock tube, calibration of the excimer source, and descriptions of two separate experiments for determining the absorption coefficient at 193 nm.

Two types of absorption coefficient determination experiments were performed: those in which only the fractional transmission of the excimer pulse was measured, and those in which the products of photolysis were monitored using narrow-line laser absorption. The fractional transmission experiments were done with the three absorbing species O_2, NH_3, and H_2O. The narrow-line laser diagnostic experiments were done to determine the product yield of OH from H_2O and to demonstrate quantitatively the yield of NH_2 from NH_3. Both the H_2O and NH_3 experiments were performed with the probe laser coaxial with the excimer beam (sidewall excimer illumination). The NH_3 experiments were also done with the laser diagnostic perpendicular to the excimer beam (endwall excimer illumination).

Description of shock tube

The shock tube used was stainless steel, 6.1 m long, 14.3 cm in diameter. The 2.4 m driver, which was 5 cm dia, diverged through a 30 cm transition section after the diaphragm station to the full driven-section diameter. The system could be baked to 350 K and was turbo-pumped (Varian VT1000). All mechanical pumps were protected with MDC zeolite sieves. The center of the view ports in the reflected section were 20 mm from the end wall. The ultimate pressure and the combined leak and outgassing rate were 9×10^{-7} torr and 1.2×10^{-6} torr/min, respectively. A driven-section isolation valve was used to reduce exposure to the atmosphere during diaphragm changes.

The stainless steel mixing assembly had a 22 l. volume with magnetic stirring and could be turbo-pumped. Pressures in the mixing assembly and the driven section were measured with a Baratron 310CHS-1000 head with a 170 M controller or with a Wallace and Tiernan FA145 (-30 to 170 in. Hg) pressure gauge. The gases used in these experiments were from Liquid Carbonic. The absorbing species O_2 and NH_3 were 99.9% pure, while the bulk carrier gas, argon, was 99.999% pure. The H_2O used was distilled. With condensible vapors, a passivation scheme was used in the shock tube to ensure that the minor constituent mole fraction was well established. This technique has been described previously.[7]

To determine shock speeds, signals from five platinum films mounted at three 610 mm intervals and one final 170 mm interval were used. The separation in time of these signals was measured with four Hewlett–Packard 5314A universal counters. The shock speeds over these intervals were measured accurately to within 0.1%. Shock speeds accelerated or decelerated in the test region from $-0.25\%/\mathrm{m}$ at 3000 K to $+0.5\%/\mathrm{m}$ at 1500 K. The pressure of the shocked gas was measured with a Kistler 603B1 transducer and 5004 amplifier. These pressures agreed within experimentally determined error ($\pm 2\%$) with the pressures derived from the chemically-frozen calculations used to determine the post-shock conditions. Test times determined from these pressure traces and temperature determinations using the OH scanning technique described in Chang et al[12] were always $\geqslant 2$ msec in the temperature range 3500–1500 K.

Diagnostic signals were stored with digital oscilloscopes (Nicolet model 2090 using model 206 amplifiers with 400 kHz 3 dB bandwidths). The gas mixture partial pressure measurements, the thin film time-interval measurements, and the recorded voltage measurements of the diagnostic signals were all traceable to NBS standards.

Excimer configuration and energy calibration

The 193 nm photolysis radiation was produced with a Questek model 2220 ArF excimer laser operating with stable optics. This laser produced a maximum of 200 mJ per pulse, with a typical duration of 25 nsec and a FWHM of 0.6 nm. The excimer high voltage charging circuit was triggered manually just before breaking the shock tube diaphragm, and the laser-pulse trigger was modified to respond to a trigger pulse initiated by a thin film shock arrival sensor followed by a time delay generator (Abtronics Model 200).

Three 90° turning mirrors were used to direct the beam from the excimer exit window to the shock tube. These were made of Suprasil™ with an Acton Research Corp. 193-FR45 coating and had 95% reflectivity at 193 nm and $>80\%$ transmission at wavelengths longer than 240 nm. The 180° turning mirror used in the double pass experiments was similar to the above but with a 193-FR coating.

Two excimer illumination configurations were used: sidewall illumination, in which the excimer beam entered the shock tube coaxially through the same window as the probe beam, and endwall illumination (see Fig. 1), where the expanded excimer beam entered through the endwall of the shock tube. Illustrations of the beam overlap and shock tube location have been presented previously.[7] A 500 mm f.l. CaF$_2$ (Janos Corp.) lens was used in the sidewall illumination scheme when higher intensities were desired. In the endwall configuration, a fused silica (f.l.-300 mm) cylindrical lens was used to expand the beam to cover the shocktube-endwall window. This window

Fig. 1. Schematic of the experimental apparatus for the end-wall illumination scheme; BS, beam splitter; ND, neutral density filter; A, aperture; FP, Fabry–Perot interferometer; Det., photodetector; M, mirror; L, lens; TF, thin-film sensor.

was 10 cm wide and 2 cm high and allowed coverage of 85% of the shock tube internal diameter along the laser diagnostic beam path. The shocktube-endwall window is u.v.-grade fused silica.

Accurate measurement of excimer pulse energy distributions are not simply obtained. NBS standard techniques for the determination of excimer energies are not presently available. Because of the brevity of the excimer pulses and the limited observation volume of laser diagnostics, classical chemical actinometry methods to measure the pulse energy flux are also not easily applicable. The determination of the excimer energy per unit area into the shocked absorber gas was therefore measured using different commercial instruments which could be compared against each other.

The Questek excimer laser has an internal factory-calibrated photodetector which measures the total pulse energy accurate to ± 2.5 mJ. This is related to the Questek in-house measurement standard. The full pulse energy entering the shock tube was also measured with a Scientech 10 cm dia calorimeter which was thermally calibrated. This device requires a correction at 193 nm. Small area local energy measurements were made with a Molectron JA50HR pyroelectric joulemeter which was calibrated against the first two devices. All instruments gave energy readings within 5% of one another.

The actual excimer pulse energy per unit area at the shock tube was determined with a Molectron detector and a precision mask that was movable within the beam profile. Several excimer illumination configurations were used. Sidewall illumination with no lenses in the 2 m beam path gave approx. 10 mJ/cm² per single 100 mJ excimer pulse. A two-fold increase in power density could be achieved by adding one lens (f.l.-500 mm) to the excimer beam path. This lens helped to counteract the natural beam divergence (4×6 mrad) of the excimer. Endwall illumination produced 2 mJ/cm². This required one cylindrical lens (f.l.-300 mm) to expand the beam to the full width of the endwall window. Sufficient beam divergence in the vertical dimension existed to cover the 1.5 mm dia laser diagnostic beam. The excimer energy input per unit area was measured to be flat over the diagnostic field to within $\pm 5\%$ for all configurations.

Transmission experiments

The fractional transmission measurements were done in a standard manner. The excimer energy entering the shock tube was sampled from behind the last 95% reflective 90° turning mirror with a Molectron pyroelectric joulemeter. The exit energy from the shock tube was sampled behind the 95% reflective 180° turning mirror mounted on the shock tube. The excimer illumination profile was sampled over the same central 1.0 cm dia of the beam on both detectors. Over this diameter the excimer pulse energy per unit area was measured to be flat within $\pm 10\%$. The primary advantage of this large sampling area is that it is insensitive to small shock tube movements. The Molectron detector signal has a rapid rise with a slow exponential decay (τ approx. 1 msec). The signal-to-noise ratio in the peak determination was approx. 20:1. Background absorption in pure argon shocks resulted in a background absorption coefficient-mole fraction product of < 0.001 atm^{-1} cm^{-1}, and was indistinguishable from the noise. For each absorber, values of the mole fraction were selected, such that the excimer pulse experienced 30–60% absorption at shock temperatures. In the case of O_2, this mole fraction was typically 0.5–3%.

The absorption coefficient, k_{193}, was inferred using the two parameter non-dimensional theory described previously.[4] A calculation of radical concentration similar to this approach has been used in a study of ignition by excimer laser photolysis of ozone.[13] Under the conditions that photolysis is normally employed for kinetic studies, the photolysis-product concentration profiles can be described by two dimensionless parameters,

$$f = k_{193} ERT / (h\nu N_A), \tag{1}$$

$$g = k_{193} PX_0 L, \tag{2}$$

where k_{193} is the absorption coefficient (atm^{-1} cm^{-1}), $E/h\nu$ is the number of excimer photons per unit area (cm^{-2}), N_A is Avogadro's number (mole^{-1}), R is the universal gas constant (atm cm^3 mol^{-1} K^{-1}), and X_0 is the initial mole fraction of the absorbing species, i.e., prior to photolysis.

The quantity g is the initial optical depth. The quantity f is the fraction of absorber molecules that undergo absorption at the leading edge of the absorber; it is proportional to the absorption

coefficient and the number of incident photons. The ratio f/g is the number of photons in the excimer pulse divided by the number of absorbers in the path. Small values of g are those where the absorber is optically thin. Small values of f are those where the $E\,k_{193}$ product is small and thus the fractional conversion to product is small.

If both f and g are small, the product profile X_P will be uniform (a desirable condition in kinetic studies) and assuming unity quantum yield,

$$X_P = fX_0. \qquad (3)$$

For large values of f or g, a full numerical calculation is necessary to predict the concentration distribution of photolysis products and the resultant absorption of the excimer pulse.[4]

The determination of k_{193} from the transmission measurements was done using an iterative procedure. By using an estimate of k_{193}, the fractional transmission I/I_0 was predicted and compared with the measured I/I_0, derived from a excimer pulse of energy density, E, transiting a pathlength, L, of shock-heated gas, with the mole fraction, X_0, of an absorber. The measured shock speed gave values for T_s and P_s, the shock-heated temperature and pressure. By a converging iterative procedure, a k_{193} value was found which gave agreement between the measured and the predicted value of the transmission.

Errors in this determination of k_{193} are primarily due to the scatter in the measured value of I/I_0. Other sources of error include the uncertainty in vibrational temperature and in the magnitude of product or impurity absorption. In the case of reflected shock measurements of O_2, the delay in the firing of the excimer pulse, typically $300\,\mu\text{sec}$, was chosen to allow time for full vibrational relaxation.[14] For incident shock measurements of O_2, the excimer pulses occurred immediately behind the incident shocks, and thus the O_2 vibrational population was considered frozen in the ground state. In the cases of H_2O and NH_3, vibrational equilibrium occurred very rapidly. However, in photolysis experiments at temperatures near 3000 K, it was necessary to calculate with a detailed kinetic model the actual mole fraction of the absorber at the time of the excimer pulse. In these experiments, the direct products of photolysis, OH, H, NH_2, and O, created no significant absorption at 193 nm.[15]

Narrow-linewidth absorption laser diagnostic

The second set of experiments involved the use of an absorption diagnostic to measure the products of photolysis. The schematic of the experimental apparatus is shown in Fig. 1. For the experiments performed with water, typically 1% H_2O was photolyzed using 10 mJ/cm^2 in the temperature and pressure regimes of 1500–3200 K and 0.9–1.2 atm. This resulted in OH and H photolysis-product concentration profiles that were typically 50 ppm and this profile was uniform in the direction of the diagnostic beam within several percent. The OH vibrational population under these conditions is rapidly thermally equilibrated.[16]

The narrow-linewidth absorption laser diagnostic has been described previously.[17,18] This diagnostic utilized a Spectra-Physics model 380 ring dye laser pumped by a Spectra-Physics model 171 argon ion laser. The ring dye laser was run with Rhodamine 590. The single-mode structure was verified with a Spectra-Physics Model 470, scanning interferometer with a free spectral range of either 2 or 8 GHz, and the output wavelength was measured with a Burleigh WA-10 wavemeter. The NH_2 was detected by absorption at 597.375 nm, using the $A^2A_1 \leftarrow X^2B_1$ (090←000) $\Sigma^P Q_{1,N}(7)$ transition. For OH, output of the ring dye laser was intra-cavity doubled with an $AD*A$ crystal. The OH was detected by absorption at 306.687 nm, using the $A^2\Sigma^+ X^2\Pi$ (0,0) $R_1(5)$ transition.

The diagnostic beam was directed 6 m to the shock tube and focussed to a diameter of < 1 mm. Before entering the shock tube, the absorption laser beam was split into a reference beam and a probe beam which traversed the shock tube. The reference and probe beam were balanced (in the case of NH_2) with neutral density filters or (in the case of OH) by sampling partial reflections off a beam splitter. The two beams were detected by EG&G silicon photodiodes (model UV100BQ) and amplified by matched amplifiers with a 250 kHz 3 dB bandwidth. The probe and reference signals as well as the different signals were stored on the Nicolet digital oscilloscopes. Based on the residual noise of the different signal, the minimum useful absorption signal was typically 0.1% with a S/N of 2.
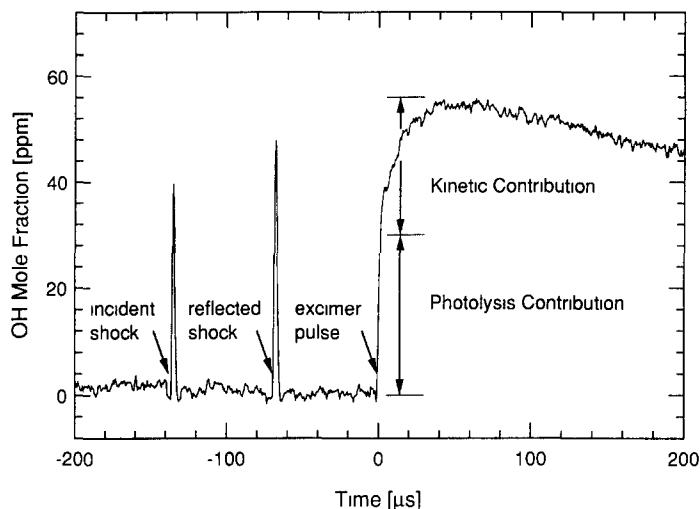
Fig 2 OH mole fraction vs time, an experimental sample at shock conditions, $P_5 = 1.21$ atm, $T_5 = 1790$ K, 1 81% H_2O in Ar, the first spike is a result of beam steering by the incident shock, the second spike is produced by the reflected shock beam steering, the contributions to the long-time OH mole fraction plateau from photolysis and kinetics are shown

Several materials have been tried for shock tube side windows in the sidewall illumination scheme, and their suitability for use with a polarized laser diagnostic varied. CaF_2 windows are preferred in the absence of coincident excimer illumination, but have been found to color-center with even minimal excimer exposure. MgF_2 windows exhibit slight birefringence, and this in combination with even minimal shock tube vibration produced large variations in the effective window transmission. Ultraviolet grade fused silica (several suppliers) has given the most success with the least complications for coaxial sidewall photolysis.

The absorption coefficient for H_2O can be inferred from the photolysis yield of OH and its subsequent kinetics. The O/H kinetics are well understood under the conditions of these experiments and the full mechanism is described by Warnatz.[19] The product concentrations at long times (5–40 μsec) predicted by this mechanism are relatively insensitive to the early post-photolysis non-equilibrium kinetics because of the lack of strong OH loss mechanisms. The resultant long time concentration plateaux of OH are then made up by a contribution by the initial photolysis yield, $(OH)_0$, and a contribution by kinetics, primarily by the reaction $H + H_2O \rightarrow OH + H_2$.

The photolysis yield was found by fitting the measured OH profiles with the above mechanism and varying the initial photolysis yields of $(OH)_0$ and $(H)_0$. For the small photolysis-product concentrations produced in these experiments, the absorption coefficient for H_2O can be determined using Eq. (3). An example of the measured OH concentrations is shown in Fig. 2 and the inferred values for the absorption coefficient for H_2O are shown in Fig. 7.

The NH_3 photolysis data are a demonstration of NH_2 product yield. These data were also used in a study where the absorption coefficient of NH_2 was determined.[7] In the photolysis of NH_3, initial concentrations similar to H_2O were used. However, because of the larger absorption coefficient of NH_3, this resulted in approx. 300 ppm NH_2 being produced in a nonuniform product profile. To alleviate this problem endwall illumination was used. This resulted in a NH_2 product concentration profile which was uniform along the diagnostic beam path. An example data trace for NH_2 with endwall illumination is shown in Fig. 3.

RESULTS AND DISCUSSION

For each absorbing species, the absorption coefficient is a function of the incident wavelength and of the quantum states of the absorber. The experimentally measured k_{193} is an integral over the multiple absorption transitions weighted by the excimer spectral intensity distribution. This multiplicity of absorption transitions provides a distribution of product states, followed usually by
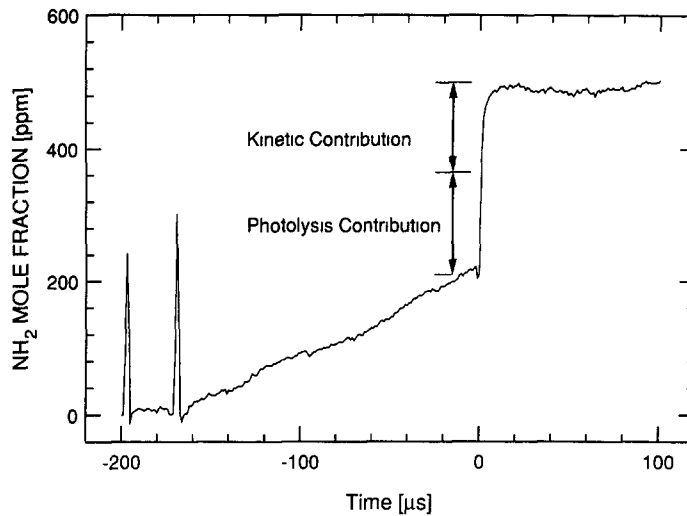
Fig. 3. NH$_2$ mole fraction vs time, experimental sample Shock conditions, $P_5 = 1\ 07$ atm, $T_5 = 2195$ K, 1 0% NH$_3$ in Ar, the ramp in the mole fraction from -170 to $0\ \mu$sec is a result of NH$_2$ formed by NH$_3$ pyrolysis, the contributions to the long-time [NH$_2$] mole fraction plateau from photolysis and kinetics are shown

rapid equilibration to a thermalized distribution. The absorption coefficients of the three species O$_2$, NH$_3$, and H$_2$O are discussed separately below.

Absorption coefficient of O$_2$

Photo-excitation of ground state O$_2(^3\Sigma_g^-)$ by 193 nm excimer radiation primarily yields the $B(^3\Sigma_u^-)$ state. This state predissociates to O($^3P_2$) + O($^3P_2$) with near 100% efficiency.[21] A full discussion of spectral absorption coefficients near 193 nm as they apply to O$_2$ is found in Lee and Hanson.[20] Their work takes into account the predicted absorption coefficients for all the significant absorbing lines in the Schumann–Runge band that lie within the bandwidth of the ArF excimer output. A verification of their predictions based on fluorescence measurements in a heated air torch at temperatures up to 1200 K is found in Lee et al.[8]

Following Lee and Hanson,[20] the excimer spectral distribution can be calculated after it has travelled through 2 m of room temperature air. This variation in intensity as a function of wavelength, shown in Fig. 4, is applicable for all three absorption species studied in this work. Because of the lack of fine structure at the sub-nanometer scale in the absorption bands of H$_2$O and NH$_3$, specific variations in the excimer intensity do not alter any of the conclusions drawn about these two species.

The rotational populations in O$_2$ vary smoothly at high temperatures, and the transitions from these levels are widely distributed over the bandwidth of the excimer. We assume, therefore, that the absorption coefficient measurements made at high temperatures with the variation in excimer energy distribution shown in Fig. 4, should also be a fair representation of those O$_2$ absorption coefficients for an excimer beam without intermediate room temperature air absorption. This assumption was examined in a test calculation done at 2278 K where the effective absorption coefficient of an excimer beam with 2 m of air was within 3% of that calculated without the intermediate air path.

The effective absorption coefficient averaged over the linewidth of the excimer laser can be strongly affected by bleaching. Bleaching is selective hole burning in the excimer wavelength profile by strongly absorbing lines which results in an average absorption over the excimer bandwidth that does not scale exponentially. An absorption coefficient is only meaningful in the non-bleached limit (i.e., weakly absorbing). At high absorber pressures, the effective absorption coefficient begins to decrease with increasing values of the $X\ P\ L$ product (mole fraction–total pressure–pathlength product). Bleaching is weakly dependent on pressure broadening as well.[20]
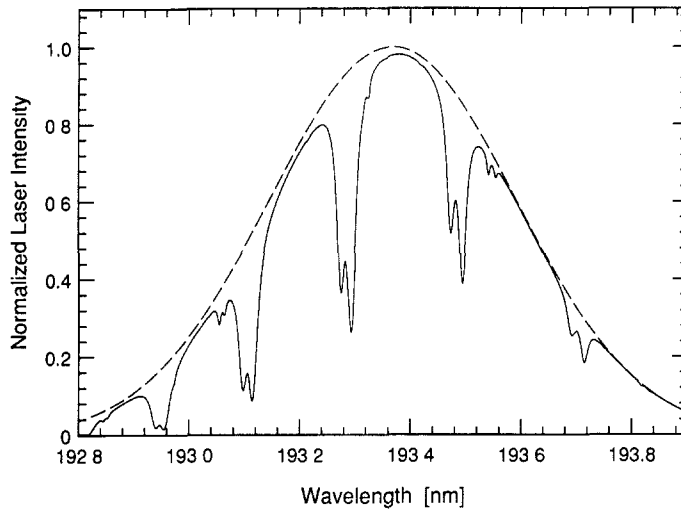
Fig 4 ArF excimer normalized laser intensity vs wavelength —, Intensity of beam after passage through 2 m of standard atmosphere, ---, intensity of beam at exit window of excimer

The experimental data and the calculations from the model of Lee and Hanson are shown in Fig. 5. The data and the model can be divided into two groups: those where selective bleaching of the excimer wavelength profile by a large oxygen partial pressure is significant and those where it is not (the optically thin case). The Lee and Hanson optically thin calculation can be used for photolysis experiments in shock tubes. It is well described by the following polynomial in the temperature range from 1000 to 3500 K:

$$k_{O_2} = -0.9854 + 1.514 \times 10^{-3} \times T - 2.812 \times 10^{-7} \times T^2 \, (\text{atm}^{-1} \text{cm}^{-1}). \tag{4}$$

It is accurate within 10% for total pressures of 1 atm or below (which influence absorption line widths) and overall extinction coefficients (the product of total pressure, absorber mole fraction, path length, and absorption coefficient) as large as 0.2.
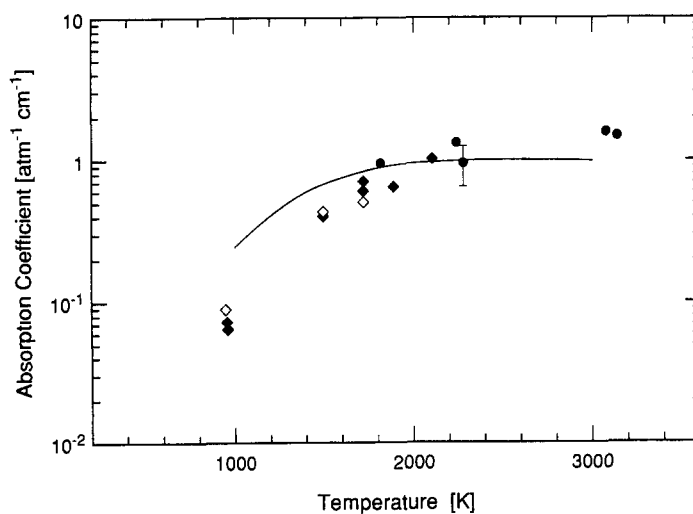
Fig 5 Absorption coefficient of O_2 vs temperature. ●, Reflected shock transmission data at O_2 concentrations where bleaching of the excimer beam by the shock heated gas does not have a significant effect on the absorption coefficient; —, Lee and Hanson[20] model calculations for optically thin case; ◆, incident and reflected shock transmission data with elevated O_2 concentrations where bleaching of the excimer profile in the shocked gas has an effect on the effective absorption constant, ◇, Lee and Hanson model calculations for typical data including the effect of bleaching
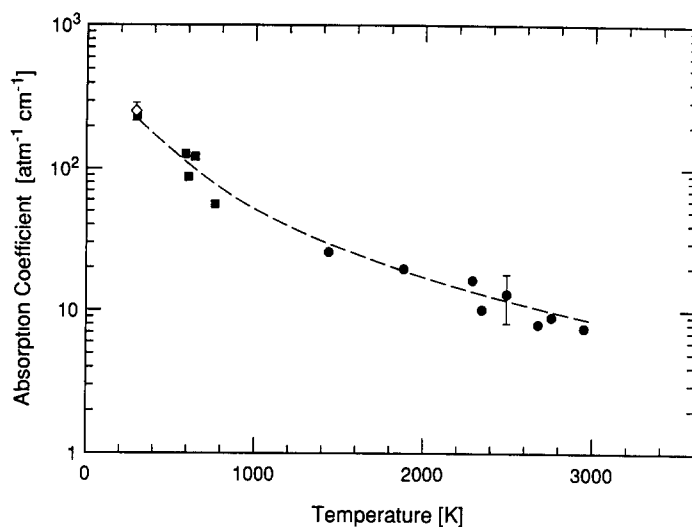
Fig. 6 Absorption coefficient of NH_3 vs temperature. — — —, Vibrational model, Eq. (5); ■, reflected shock transmission data; ◇, incident shock transmission data; ●, Watanabe[25] room temperature data.

The temperature dependence of the absorption coefficient is a result of significant photo-excitation of the vibrationally excited states. The greatest contribution to the absorption coefficient is expected from the 1st, 2nd, and 3rd vibration states, with similar absorption coefficients from each vibrational level.

The optically thin transmission experiments were performed in the reflected shock regime with O_2 mole fraction of 1 or 2%, pressure between 1.3 and 1.0 atm, and temperatures between 1700 and 3100 K. The transmission experiments which have significant bleaching were performed in the incident or reflected shock regime with between 10 and 100% O_2, at pressures between 0.4 and 1.7 atm and at temperatures from 900 to 2000 K. In agreement with calculations, the experimentally determined values in the cases with bleaching give smaller values of the absorption coefficient than observed in the optically thin limit. The slight divergence from the prediction of Lee and Hanson above 3000 K may be due to interference absorption by shock tube impurities.

Absorption coefficient of NH_3

Haak and Stuhl[22] have described the ArF excimer photolysis of NH_3. The largest absorption is from the $v_2 = 0$ anti-symmetric vibration mode to the $NH_3(A\,^1A_2'', v_2' = 6)$ upper state. This upper state dissociates to vib-rotationally excited $NH_2(X)$ and an H atom. The product energy distribution indicates that the $NH_2(X)$ carries internal energy and that the H atoms have excess translation energy. This path has a quantum efficiency of approx. 97%. 2.4% of the NH_3 is converted to $NH_2(A) + H$.[23] Less than 0.8% goes to $NH(a\,^1\Delta) + H_2$. Various two and three photon events are possible but because the incident power per unit area is only 0.12 MW/cm^2 these are considered to be insignificant.

The spectral rotational structure is diffuse even at supersonic jet-cooled temperatures, 10 K, in NH_3.[24] These broad features result in an absorption coefficient that is smoothly varying and constant to within 20% over the entire excimer linewidth.

The transmission data for NH_3 were taken in three ranges. (1) Unshocked pure ammonia at 300 K was measured at several pressures below 1 atm. (2) Absorption in incident shocks between 600 and 1500 K at approx. 0.4 atm was measured. (3) Absorption in reflected shocks was measured in 0.4% NH_3 at pressures between 1.3 and 1.0 atm in the temperature range 1900–3000 K. The measured values of k_{193} for NH_3 are shown in Fig. 6.

An increase in the vibrational energy in the NH_3 from shock heating results in a decrease in the near resonant absorption occurring from the $v_2 = 0$ ground vibrational state. The temperature variation in absorption coefficients appears to follow the population of the ground v_2 vibrational
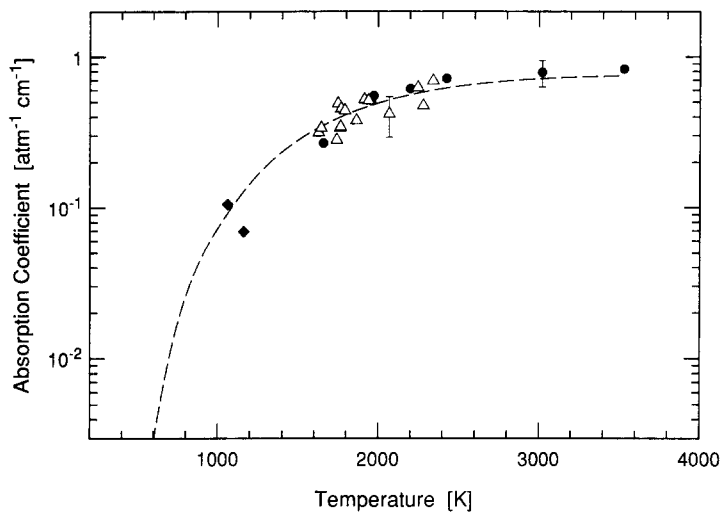
Fig. 7. Absorption coefficient of H_2O vs temperature. ---, Vibrational model of Eq. (6); ●, reflected shock-transmission data; ◆, incident shock transmission data; △, data derived from OH photolysis yields.

state and can be expressed as

$$k_{193}(NH_3) = k_0 f(v_2 = 0)(300/T) \tag{5}$$

where $f(v_2 = 0) = [1 - \exp(-1370/T)]$ and the best-fit value of k_0 is 230 ($\pm 15\%$) (atm^{-1} cm^{-1}).

The room temperature value of the u.v. absorption coefficient for NH_3 has been established by Watanabe,[25] and the current data are in good agreement with this previous work. Various workers,[26] have performed FPST work with NH_3, but have not published high-temperature absorption coefficients. Early studies by Michel and Menon[9] of shock-heated NH_3, were performed at three longer wavelengths: 222.5, 230.0, and 240.0 nm. They observed the absorption coefficient increasing with temperature. This is not inconsistent with the present work as they attributed their observation to transitions from the vibrationally excited states $v_2'' > 0$ whose population would increase with temperature.

Absorption coefficient of H_2O

The absorption of 193 nm radiation by H_2O is in the first absorption band $X^1A_1 - A^1B_1$. This upper state decomposes to $OH(X^2\Pi)$ and $H(^2S)$.[15] Room temperature H_2O does not dissociate markedly at 193 nm, and we have found no data for the temperature dependence of the absorption coefficient at this wavelength.

Early work on the temperature dependence of the absorption coefficient of H_2O in the i.r. for CO_2 cw laser wavelengths in a shock tube was performed by Krech and Pugh.[27] Early FPST work using H_2O was performed by Ernst et al[2] as well as by Michael and Sutherland.[28]

The present state of understanding of this process is reviewed by Andresen and Schnike.[10] Their study of the first absorption band is a comparison of the experimental and theoretical studies on a state-to-state basis. Photodissociation of H_2O is well understood on the basis of the known potential energy surface for the excited state and rigorous dynamic calculations including all degrees of freedom. A complete description of the process can now be obtained and it is possible to predict state-to-state cross sections for all initial H_2O and final OH quantum states, and all photolysis wavelengths.

Work by Andresen and Haüsler[11] performed at 157 nm indicates that the excess energy of the products and is distributed as: 88% translational, 10% vibrational, and 2% rotational energy. Similar results are expected at 193 nm. Infrared measurements by Andresen et al[29] indicate that the excited antisymmetric stretch mode has almost 500 times the absorption cross-section of H_2O in the vibrational ground state and is the dominant absorption mode.

The H_2O data are shown in Fig. 7. Transmission data were acquired in the temperature range from 1700 to 3500 K, at a pressure of approx. 1.2 atm and with 0.9–1.8% H_2O. The absorption

coefficients calculated from the OH photolysis yields were determined in the temperature range from 1700 to 2400 K.

It is not necessary to sum over the specific rotational states in order to synthesize the total absorption cross-section. The temperature dependence of the absorption coefficient in our experiment can be approximated by assuming proportionality to the product of the $v_3 = 1$ vibrational population and $1/T$. Thus

$$k_{193}(H_2O) = k_0 f(v_3 = 1)(300/T) \tag{6}$$

where f is the Boltzmann fraction in the first excited antisymmetric stretch mode, $f(v_3 = 1) = x(1 - x)$ and where $x = \exp(-5400/T)$, and the best fit value of k_0 is 51.3 ($\pm 15\%$) ($atm^{-1} cm^{-1} K$). There is good agreement between both types of data and the simple $f(v_3 = 1)$ model of the absorption coefficient.

CONCLUSION

The use of an excimer-laser photolysis-source provides extended capability for radical production in a shock tube beyond that of flashlamp methods. It allows significant improvements in wavelength selectivity, brevity of pulse length, and spatial distribution of radiation. Measurements of high-temperature absorption coefficients of the type reported here will permit quantitative prediction of radical production in excimer photolysis. As shown here, O_2 can be used as a predictable source of O atoms, H_2O as a source of OH and H, and NH_3 as a source of NH_2 and H.

Measured values are presented for k_{193} by two methods for temperatures up to 3500 K for the species O_2, NH_3, and H_2O. Satisfactory fits for the absorption coefficients vs temperature can be formed by simple vibrational population models. These fits are consistent with the expected dominant absorption transitions.

REFERENCES

1. J. V. Michael, J. W. Sutherland, and R. B. Klemm, *Int. J. Chem. Kin.* **17**, 315 (1985).
2. J. Ernst, H. Gg. Wagner, and R. Zellner, *Ber. Bunsenges. Phys. Chem.* **82**, 409 (1978).
3. J. Sutherland and J. Michael, *J. Chem. Phys.*, to be submitted (1989).
4. D. Davidson, A. Chang, and R. Hanson, *22nd Symposium (Int.) on Combustion*, The Combustion Institute, Pittsburgh, PA, in press (1989).
5. R. Maki, J. Michael, and J. Sutherland, *J. Phys. Chem.* **89**, 4815 (1985).
6. K. Thielen and P. Roth, *20th Symposium (Int.) on Combustion*, p. 685, The Combustion Institute, Pittsburgh, PA (1984).
7. K. Kohse-Höinghaus, D. Davidson, A. Chang, and R. Hanson, *JQSRT* **42**, 1 (1989).
8. M. Lee, P. Paul, and R. Hanson, *Opt. Lett.* **11**, 7 (1986).
9. P. Menon and K. Michel, *J. Phys. Chem.* **71**, 3280 (1967).
10. P. Andresen and R. Schinke, in *Molecular Photodissociation Dynamics, Advances in Gas Phase Photochemistry and Kinetics*, Chap. 3, p. 61, M. N. R. Ashfold and J. E. Baggott eds., Royal Society of Chemistry, Letchworth (1987).
11. D. Haüsler, P. Andresen, and R. Schinke, *J. Chem. Phys.* **87**, 3949 (1987).
12. A. Chang, E. Rea Jr., and R. Hanson, *Appl. Opt.* **26**, 885 (1987).
13. D. Lucas, D. Dunn-Rankin, K. Hom, and N. Brown, *Combust. Flame* **69**, 171 (1987).
14. R. Millikan and D. White. *J. Chem. Phys.* **39**, 3209 (1963).
15. H. Okabe, *Photochemistry of Small Molecules*, Wiley, New York, NY (1978).
16. K. Rensberger, private communication (1988); see also K. Rensberger, J. Jeffries, and D. Crosley, *J. Chem. Phys.*, in press (1989).
17. S. Salimian, Experimental Investigation of Ammonia-Nitrous Oxide Reaction Kinetics, Ph.D. Thesis (HTGL Report No. T-239), Stanford University, Stanford, CA (1984).
18. E. Rea Jr., S. Salimian, and R. K. Hanson, *Appl. Opt.* **23**, 1691 (1984).
19. J. Warnatz, in *Combustion Chemistry*, Chap. 5, W. C. Gardiner Jr. ed., Springer, New York, NY (1984).
20. M. P. Lee and R. K. Hanson, *JQSRT* **36**, 425 (1986).
21. B. Lewis, L. Berzins, J. Carver, and S. Gibson, *JQSRT* **36**, 187 (1986).
22. H. Haak and F. Stuhl, *J. Phys. Chem.* **88**, 2201 (1984).

23 V. Donnelly, A. Baronavski, and J. McDonald, *Chem. Phys.* **43**, 271 (1979).
24 V. Vaida, W. Hess, and J. Roebber, *J. Phys. Chem.* **88**, 3397 (1984).
25. K Watanabe, *J. Chem. Phys.* **22**, 1564 (1954)
26 J. Sutherland, J. Michael, and R. Klemm, *J. Phys. Chem.* **90**, 5941 (1986).
27 R. Krech and E. Pugh, in *13th Shock Tube Symposium*, p. 462, C. Treanor and G. Hall eds., SUNY, New York, NY (1981).
28. J. Michael and J. Sutherland, *J. Phys. Chem.*, in press (1989).
29. P. Andresen, G. Ondrey, B. Titze, and E. Rothe, *J Chem. Phys.* **80**, 2548 (1984).